

# A global approach to provide magnitude estimates for earthquake early warning alerts

Huseyin Serdar Kuyuk<sup>1</sup> and Richard M. Allen<sup>1</sup>

Received 4 November 2013; revised 13 November 2013; accepted 15 November 2013; published 26 December 2013.

[1] We examine five different methods to estimate an earthquake's magnitude using only  $P$  wave data for use in earthquake early warning systems. We test two input parameters: the maximum predominant period of the  $P$  wave ( $\tau_p^{\max}$ ) and the displacement amplitude of the  $P$  wave's vertical component (Pd). We apply our algorithms to 174 earthquakes  $3.0 < M < 8.0$  from California and Japan that have also been used in previous calibration studies. We also apply them to 1992  $0.2 < M < 5.7$  earthquakes that were processed by the real-time Earthquake Alarm Systems in California. We find that  $\tau_p^{\max}$  does not scale with magnitude for small earthquakes ( $M < 3$ ) and is less accurate for large-magnitude earthquakes than using Pd alone. We derive a global scaling relation between Pd and magnitude and conclude that this global relationship provides the most accurate and robust magnitude estimate. This relationship could be applied in earthquake source zones around the world. **Citation:** Kuyuk, H. S., and R. M. Allen (2013), A global approach to provide magnitude estimates for earthquake early warning alerts, *Geophys. Res. Lett.*, 40, 6329–6333, doi:10.1002/2013GL058580.

## 1. Introduction

[2] Rapid magnitude estimation is at the heart of Earthquake Early Warning Systems (EWS). The challenge is to use only a few seconds of the  $P$  wave data from a limited number of stations to quickly determine a useful estimate of the earthquake magnitude. To respond to the emergency at hand, it is crucial that these magnitude estimates are as precise as possible [Kuyuk and Allen, 2013]. For large earthquakes, substantial deviations between the estimated magnitude and the true earthquake's magnitude can lead to erroneous intensity predictions (e.g., peak ground acceleration, PGA, and peak ground velocity, PGV).

[3] In California, three algorithms provide magnitude estimation to California Integrated Seismic Network ShakeAlert EWS [Böse et al., 2013]. The first algorithm called “Virtual Seismologist” uses Pd and the peak acceleration (Pa) of the  $P$  wave [Cua et al., 2009]. The second algorithm called “Onsite” uses Pd and frequency of the  $P$  wave, ( $\tau_c$ ), which is derived from integration of displacement and velocity over a 3 s time window [Böse et al., 2009]. The third algorithm called

“ElarmS,” uses empirically derived linear scaling relationships to determine magnitude from Pd, peak velocity (Pv), and maximum predominant period ( $\tau_p^{\max}$ ) parameters. The ElarmS event magnitude is calculated by averaging the magnitudes determined independently from Pd and  $\tau_p^{\max}$  [Wurman et al., 2007]. The parameters being used by all algorithms use various versions of an amplitude and frequency measure of the  $P$  wave.

[4] In this study we focus on one amplitude and one frequency measure. These are (1) the peak displacement amplitude of the  $P$  wave (Pd) and (2) the maximum predominant period of the  $P$  wave ( $\tau_p^{\max}$ ). We derive a global scaling relationship to predict earthquake magnitude from  $P$  wave data, which can be applied to data worldwide. To derive the scaling relationship we use waveform records from past/historic earthquakes used as calibration data sets in previous studies and data from the current real-time ElarmS system running in California. Instead of using different regional scaling relationships for each individual region, we use a global data set and explore various approaches to estimate magnitude from the  $P$  wave data. We conclude that our preferred method is a new Pd-based global scaling relation that we find is more accurate and simpler than the combined Pd and  $\tau_p^{\max}$  based methods. We tested this new equation in our operational statewide ElarmS test bed at the UC Berkeley Seismological Laboratory and conclude that the new Pd method based on only  $P$  wave data information provides better estimates of earthquake magnitudes than the current scaling relationships.

## 2. Data and Analysis

[5] The maximum predominant period ( $\tau_p^{\max}$ ) of the  $P$  wave is one indicator of the size of an earthquake based on the frequency content of the signal. It is calculated in a recursive fashion from the vertical component of broadband (velocity) or strong motion (accelerometer) data within 4 s of the  $P$  wave trigger [Allen and Kanamori, 2003; Olson and Allen, 2005]. The other indicator of the magnitude of an earthquake we explore is the peak absolute amplitude of the  $P$  wave displacement (Pd), which is determined from the vertical component displacement waveform that has been filtered by a causal two-pole 3 Hz low-pass Butterworth filter and is measured in centimeters. The maximum value within 4 s of the  $P$  wave is used. In the case where the  $S$  wave arrives within 4 s of the  $P$  wave, we only use  $P$  wave data up to the  $S$  wave arrival in our analysis.

[6] We make use of “calibration” data sets used in previous studies from three different regions. The first region is Northern California (NCA) where Wurman et al. [2007] derived scaling relationships for Pv, Pd, and  $\tau_p^{\max}$  from a data set of 43 events ranging in size from  $M_L$  3.0 to  $M_w$  7.1 between 2001 and 2007. The second region is in Southern California (SCA), where Tsang et al. [2007] determined relationships for Pd and  $\tau_p^{\max}$  with a data set of 59 events (magnitude range 3.0 to 7.3)

Additional supporting information may be found in the online version of this article.

<sup>1</sup>Seismological Laboratory, University of California, Berkeley, California, USA.

Corresponding author: H. S. Kuyuk, 209 McCone Hall, University of California, Berkeley, CA 94720, USA. (skuyuk@seismo.berkeley.edu)

**Table 1.** Data Sets Used in Studies of Earthquake Early Warning Systems (EEW) for Past Studies and This Study

	Number of Events	Number of Records $\tau_p^{\max}$ , Pd, Pv	Magnitude	Scaling Relationship	Source
<i>Past Studies</i>					
NCA	42	186,161,135	3.0–7.1	$\tau_p^{\max}$ , Pd, Pv	<i>Wurman et al.</i> [2007]
SCA	59	1762,1931,~	3.0–7.3	$\tau_p^{\max}$ , Pd	<i>Tsang et al.</i> [2007]
Japan	84	2552, 2469, ~	4.0–8.0	$\tau_p^{\max}$ , Pd	<i>Brown et al.</i> [2011]
<i>This Study</i>					
NCA	32	172	3.0–7.1		
SCA	58	1702	3.0–7.3		
Japan	84	1874	4.0–8.0		
Real Time	1992	12519	0.17–5.69		
Combined	2066	16267	0.17–8.0		

between 1992 and 2003. The third region is in Japan (JAP) and includes 84 earthquakes  $4.0 < M < 8.0$  that occurred between September 1996 and June 2008 [Brown et al., 2011]. Of these earthquakes, 43 events are equal to or exceeded magnitude 6.0.

[7] In this study we exclude data when (1) an earthquake was recorded by less than three stations, (2) a station does not have both Pd and  $\tau_p^{\max}$  observations, and (3) stations that have epicentral distances greater than 250 km. In total, our combined data set includes 174 events ( $0.2 \leq M \leq 8.0$ ) and 3748 records (Table 1).

[8] We also apply our method to 1992 earthquakes from 1 May 2012 to 10 June 2013. These events were detected by the ElarmS EEWs [Kuyuk et al., 2013] and are confirmed earthquakes based on a match with the Advanced National Seismic System composite earthquake catalog within  $\pm 3$  s of the origin time and  $\pm 20$  km in epicentral distance. The magnitudes range from 0.2 to 5.7. The three calibration data sets described above are typical of those used to develop EEWs magnitude scaling relationships, i.e., all  $M > 3.0$ . This additional real-time data set provides a “real world” view of the events that any EEWs must handle, i.e., very small earthquakes in addition to the larger magnitudes that the warning system is designed for.

[9] The relationship between magnitude and epicentral distance of all the observations used in this study are shown in Figure S1, which is included in the supporting information. All Pd and  $\tau_p^{\max}$  observations are shown in

Figure 1, which immediately reveals a problem with the  $\tau_p^{\max}$  parameter in that it does not scale with magnitude for  $M < 3$  earthquakes.

### 3. Testing P Wave Scaling With Magnitude

[10] We test and compare five different methods to compute an earthquake’s magnitude from P wave data information (Table 2).

#### 3.1. Method 1: Average of $\tau_p^{\max}$ and Pd Magnitude Estimates

[11] The method takes the average magnitude from the two magnitudes estimated separately using the  $\tau_p^{\max}$  and Pd regional scaling relationships. This approach was adopted for the initial version of ElarmS [Wurman et al., 2007]. This combined approach showed superior performance results at both ends of the magnitude ( $3 < M < 7.1$ ) scale in northern California. Wurman et al. tested various weighting schemes that change linearly with earthquake magnitude, but their results showed that the simple average appears to be as good as any weighted average. However, when we include additional data from SCA, JAP, and real-time events detected across California by ElarmS, the simple linear weighting scheme is not appropriate for small earthquakes ( $M < 3$ ). When applying this linear weighting scheme to small events, we found the mean magnitude was overestimated by

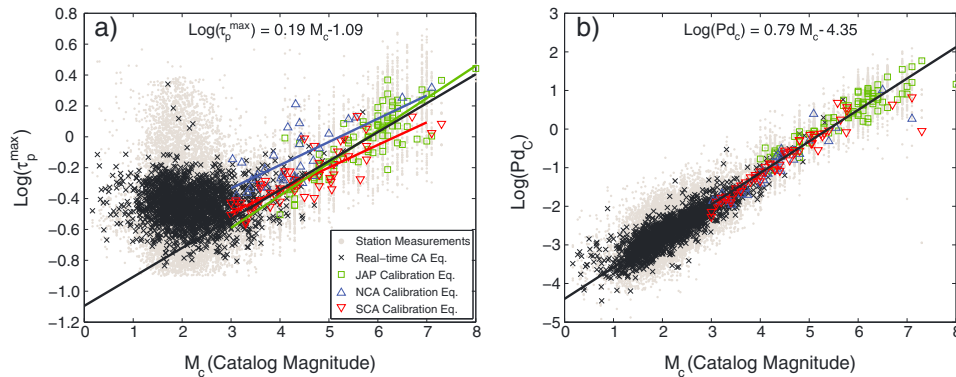


**Figure 1.** Scaling relationships between catalog magnitude and (a)  $\tau_p^{\max}$  and (b)  $Pd_c$ . Light gray dots are individual station observations for all events in study. Green squares and red and blue triangles are average values for individual earthquakes from the historic/calibration data sets from Japan (JAP), Southern California (SCA), and Northern California (NCA), respectively. Black crosses are average values for earthquakes recorded in real-time by ElarmS across California. In Figure 1a the best fit lines to the regional data sets are shown with colored lines, and the black line is the best linear fit to all the data excluding the real-time-detected earthquakes (equation shown). In Figure 1b the black line (equation shown) is the least squares multiregression fit to the entire data set and represents our preferred global scaling relationship.

**Table 2.** Comparison of Five Different Methods to Estimate Earthquake Magnitude From Only  $P$  wave Data<sup>a</sup>

	Mean( $\tau_p^{\max}$ , Pd)	Multiregression Equation (1)	Regional $\tau_p^{\max}$	Regional Pd	Global Pd (This Study, Equation (2))
All	$-0.45 \pm 0.76$	$-0.23 \pm 0.40$	$-0.87 \pm 1.41$	$-0.02 \pm 0.32$	$-0.01 \pm 0.31$
$M < 3$	$-0.57 \pm 0.81$	$-0.29 \pm 0.42$	$-1.10 \pm 1.51$	$-0.03 \pm 0.31$	$-0.03 \pm 0.31$
$M > 3$	$0.09 \pm 0.46$	$0.03 \pm 0.30$	$0.15 \pm 0.77$	$0.02 \pm 0.35$	$0.06 \pm 0.34$
$M > 5$	$-0.02 \pm 0.43$	$0.05 \pm 0.41$	$-0.01 \pm 0.60$	$-0.02 \pm 0.45$	$-0.02 \pm 0.43$

<sup>a</sup>Table values are the mean error, which is the catalog minus the estimated magnitude (residual). Also listed are the standard deviations in the error.

0.57 magnitude units, and for all earthquakes in the data set the average overestimation is 0.45 magnitude units.

### 3.2. Method 2: Multiregression Analysis

[12] We next test a multiregression approach that considers both  $\tau_p^{\max}$  and Pd at the same time. The idea behind this approach is to estimate magnitude with one equation rather than averaging the magnitude estimates produced separately from  $\tau_p^{\max}$  and Pd. The regression equation is

$$M = 4.76 + 0.431 \log(\tau_p^{\max}) + 1.47 \log(E) + 0.99 \log(\text{Pd}) \quad (1)$$

where  $E$  is epicentral distance (km). This method is preferred over Method 1 because the magnitude overestimation is reduced to 0.23 and the standard deviations are reduced to 0.40 for all events (Table 2, column 2).

### 3.3. Method 3: Regional Scaling Relationships for $\tau_p^{\max}$ (only) Versus $M$

[13] For our three target study regions (NCA, SCA, and JAP) there are three slightly different scaling relationships between  $\tau_p^{\max}$  and  $M$  (colored lines on Figure 1a). We use these regional scaling relations in an effort to obtain the most accurate magnitude estimates from  $\tau_p^{\max}$  alone to compare with the other approaches. These scalings provide poorer results with a mean error of 0.87 and a standard deviation of 1.41 (Table 2). We also determined a single global regression relation for  $\tau_p^{\max}$  versus  $M$  (black line and equation on Figure 1a), but it does a very poor job giving a mean magnitude error of 1.44 and standard deviation of 0.87.

### 3.4. Method 4: Regional Pd or Pv versus $M$ Scaling

[14] There are a total of five regional amplitude (Pd or Pv) versus  $M$  relations for our three study regions. Each region has a Pd versus  $M$  relation. In addition, there are two Pv versus  $M$  relations for different types of accelerometers in northern California [Wurman *et al.*, 2007]. Again, we use these relations to measure the accuracy of Pd/Pv-only approach when compared to the other methods described. In this work we find that these methods that use only amplitude as input (i.e., not  $\tau_p^{\max}$ ) produce results with a minimal average error in the magnitude of 0.02 and a standard deviation of 0.32.

### 3.5. Method 5: Global Pd Versus $M$ Scaling

[15] Our work shows that Pd correlates with magnitude even for smaller earthquakes (Table 1; Figure 1b). Here we propose using a global Pd-Magnitude scaling relationship derived using a linear best fit to the combined data sets (i.e., calibration data sets from three regions and real-time data from California). The best fit regression relation for the global data set is

$$M_{\text{Gpd}} = 1.23 \log(\text{Pd}) + 1.38 \log(E) + 5.39 \quad (2)$$

where  $E$  is the epicentral distance in kilometers and Pd is in centimeters. Using this relation, we can also correct Pd observations for epicentral distance in order to plot the corrected Pd, Pd<sub>c</sub>, versus catalog magnitude  $M_C$  and find the best fit relation (Figure 1b)

$$\log(\text{Pd}_c) = 0.79M_C - 4.35 \quad (3)$$

[16] It has the smallest average magnitude error (0.01) and also the smallest standard deviation (0.31) in the magnitude errors. This new scaling relationship has a 0.95 correlation coefficient ( $R$ ). Estimating  $R$  individually by region, the correlation drops to 0.93, 0.93, 0.94, and 0.89 for the JAP, NCA, SCA, and real-time California regions, respectively.

### 3.6. Summary of Methods Tested

[17] We find that  $\tau_p^{\max}$  methods (Table 2, columns 1, 2, and 3) tend to overestimate earthquake magnitudes. For small-magnitude ( $M < 3$ ) events, the regional  $\tau_p^{\max}$  scaling overestimates earthquake magnitude by 1.1 unit with a  $\pm 1.5$  standard deviation. For larger events, multiregression gives slightly underestimated magnitudes and small standard deviations. However, the smallest RMS error is acquired when using global scaling Method 5 that uses only Pd as input. The errors and standard deviations for all the methods also have a dependency on magnitude (Figure 2). The average error and standard deviation for each method in each 0.5 magnitude bin is shown. The Pd-based scaling relationships (Figures 2b, 2d, and 2e) have minimum dependency on magnitude, i.e., they do a reasonable job for both large and small earthquakes. The  $\tau_p^{\max}$  approach (Method 3) has a mean residual close to zero for  $M > 3$  events (the reason it was adopted for early warning in the first place) but has mean residual of 1.10 for  $M < 3$  (causing an overestimation of magnitude) and has standard deviation twice as large as the Pd-based methods (Figure 2c).

## 4. Discussion

[18] A study of data from a deep South African mine by Lewis and Ben-Zion [2008] is one of the few studies that previously investigated  $\tau_p^{\max}$  scaling for small-magnitude earthquakes ( $0 < M < 4$ ). They do show that  $\tau_p^{\max}$  scales with magnitude, but the measurement is made is at higher-frequency band than used here. The reason that the  $\tau_p^{\max}$  observations we make here for  $M < 3$  earthquakes do not scale with magnitude is due to our choice of real-time filtering. Our 3 Hz low-pass filter removes higher frequencies that are more prevalent for smaller earthquakes; thus, the  $\tau_p^{\max}$  value is not as small as it should be. In the Wurman *et al.* [2007] study they selected the 3 Hz low-pass frequency filter scheme to optimize the magnitude estimates for earthquakes with  $M > 3$ . This filter therefore works appropriately for the larger earthquakes, but it causes an overestimation of earthquake magnitude for the smaller earthquakes

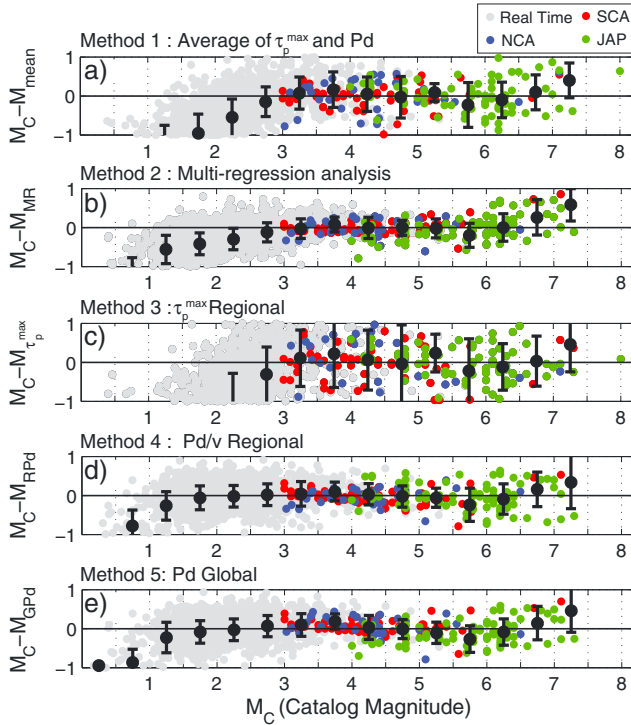


**Figure 2.** Dependency of errors in estimated magnitude as a function of the catalog magnitude. Residuals are calculated by subtracting estimated magnitude from catalog magnitude ( $M_c$ ). Only the event averages are shown. Light gray dots are earthquakes recorded in real time by ElarmS across California. Green, red, and blue dots are residuals of earthquakes from Japan (JAP), Southern California (SCA), and Northern California (NCA), respectively. Black circles and error bars show the average magnitude error and standard deviation of data within 0.5 magnitude bins. (a) Magnitudes estimated separately from  $\tau_p^{\max}$  and Pd ( $M_{\text{mean}}$ ) and these two values are averaged to obtain a final magnitude estimate. (b) Magnitudes estimated using a multiregression analysis that uses  $\tau_p^{\max}$  and Pd (equation (1)). (c) Magnitude estimated using  $\tau_p^{\max}$  regional scaling relationships. (d) Magnitude estimated using Pd/v regional scaling relationships. (e) Magnitude estimated using our preferred global Pd scaling relation (equation (2)).

( $M < 3$ ). The conclusion is therefore that  $\tau_p^{\max}$  can be used to indicate the magnitude of an earthquake, but the magnitude sensitivity range is dependent on the band-pass filter initially applied. A multistage approach could therefore be developed where  $\tau_p^{\max}$  is measured at different frequencies to determine the magnitude estimate.

[19] In light of the simplicity of the single global Pd scaling relation that we have observed here (Figure 1b) and the fact that it provides better magnitude estimates than  $\tau_p^{\max}$  anyway, we recommend simply using Pd scaling. The fact that the single relation also does better than the individual regional efforts also suggests that this relation can be applied to other earthquake source zones around the world. The downside of using Pd is that Pd is sensitive to epicentral distance while  $\tau_p^{\max}$  is not. When a seismic network is being used in the source region, good location estimates are available with a few triggers. ElarmS does not issue an alert until four  $P$  waves have been detected so this is not a concern

provided that the event is within the seismic network and the triggers are accurate. In addition to providing good locations, requiring four triggers also reduces false alarms.

[20] The magnitude estimates based on Pd observations alone (Method 5) do indicate a saturation effect at  $M \sim 7$ . This causes an underestimation of magnitude for events larger than  $M7$ . We suggest there might be two reasons for this problem. Limited data for some of these large events is one problem (Figure 3). This includes (1) having only a few records, (2) only having data from larger epicentral distances, and (3) not having a very good azimuthal coverage. For the Tokachi-oki offshore earthquake ( $M=8$ ) the six closest stations are relatively far away at 231–280 km (Figure 3). Similarly, in California for the Gorda Plate ( $M=7.1$ ) earthquake, the source-to-station distance range is 163–193 km. Likewise, the azimuthal coverage for both events is small. For both events, the large station distances and limited azimuthal coverage is because they were offshore, and the magnitudes are significantly underestimated (Figure 3). In our compiled data set, the smaller earthquakes ( $6.5 < M < 7.0$ ) do not have these near-field and azimuthal recording deficiencies.

[21] The other explanation for the saturation (Figure 3) is related to the fundamental physics of earthquake rupture. We are only using 4 s of data, which is similar to the expected duration of an  $M7$  rupture. Also, the amplitude of ground motion in the near field is expected to saturate for large-magnitude events. For these reasons it is important to develop additional methodologies to better characterize large-magnitude events ( $M > 7$ ). Such development is underway using both seismic and geodetic methods. One approach is to expand the length of the  $P$  wave window used [Colombelli *et al.*, 2012]. The “FinDer” algorithm estimates the finite extent of rupture using seismic observations [Böse *et al.*, 2012]. Emerging approaches using GPS-based earthquake early warning systems will also compliment seismic methods [Allen and Ziv, 2011; Colombelli *et al.*, 2013].

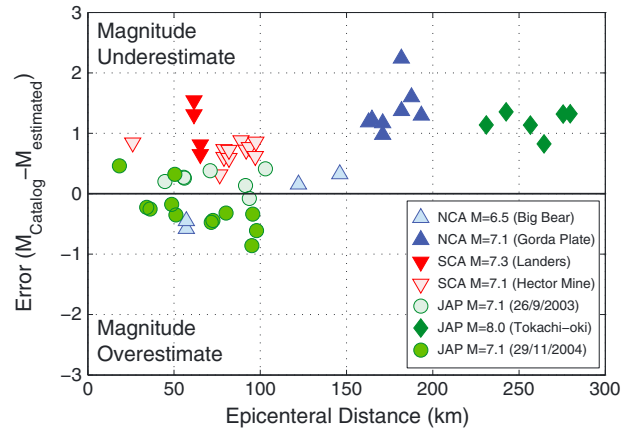


**Figure 3.** Magnitude errors versus epicentral distance for the largest earthquakes in our data set ( $M > 7.0$ ) where  $M_{\text{estimated}}$  is computed using our preferred global Pd relation (equation (2)). Earthquakes that lack near-field recordings, such as the offshore Gorda Plate and Tokachi-oki events, tend to underestimate magnitude. Earthquake recorded over limited distance ranges (e.g., Landers and Hector Mine) have larger errors than earthquake recorded at wider distance ranges (e.g., Big Bear; JAP  $M=7.1$ , 26 September 2003; and JAP  $M=7.1$ , 29 November 2004).

When the point source/Pd-based magnitude estimates are large, say larger than 6, the finite source algorithms can be interrogated for evidence of extended fault rupture.

[22] Wurman *et al.* [2007] proposed five different equations to determine magnitude that depend on the recording channel. They found that the scaling relationship between magnitude and Pd had different slopes for the velocity and acceleration data. Tsang *et al.* [2007] and Brown *et al.* [2011], on the other hand, adopted one relationship each for southern California and Japan, respectively. Although the slope is different for JAP, the slope for SCA and NCA are very similar. Here we suggest that for earthquakes up to magnitude 7, the new Pd versus  $M$  methodology we present (equation (2)) should be used to estimate magnitude for EEWS. We find no evidence that regional Pd scaling relations are better than simply using this global  $M_{\text{GPD}}$  approach. This new method removes the complexity of the regional scaling relationship. We favor this global Pd versus  $M$  method because it is simpler than other methods and has a uniform dependency on magnitude. Equation (2) has now been implemented into ElarmS and as such, contributes to California's ShakeAlert EEWS [Böse *et al.*, 2013].

## 5. Conclusion

[23] We explored five different methods to estimate earthquake magnitude from  $P$  wave data for use in EEWS. We tested these methods on calibration data sets from earthquakes of magnitude 3.0–8.0 recorded in California and Japan. In addition to the historic calibration data, we also tested them with data recorded over a 1 year period 2012–2013 by the real-time implementation of the ElarmS method for EEWS currently implemented across California. These real-time data provided an opportunity to test the methods on smaller earthquakes ( $0.1 < M < 3.0$ ) that have been largely ignored in previous studies. Comparison of  $\tau_p^{\text{max}}$  and Pd-based magnitude estimation methods indicate that Pd scaling is observed for all earthquakes, whereas the frequency filtering required for the  $\tau_p^{\text{max}}$  observation results in sensitivity to only a limited frequency range ( $M > 3.0$  for the implementation tested here). We conclude that the best approach to derive EEW magnitude estimates is to use only the Pd parameter and the global scaling relationship  $M_{\text{GPD}} = 1.23 \log(\text{Pd}) + 1.38 \log(E) + 5.39$ . This new method provides smaller RMS errors than existing regional methods based only on Pd. Our results show that this new technique using only Pd information is robust and delivers the most accurate global magnitude estimates for earthquakes up to  $M \sim 7$ . Above  $M7$  a saturation effect is observed and the application of other finite source type methods is needed.

[24] **Acknowledgments.** This work is funded by USGS/NEHRP award G12AC20348 and by the Gordon and Betty Moore Foundation through grant GBMF3024 to UC Berkeley.

[25] The Editor thanks Aldo Zollo and an anonymous reviewer for their assistance in evaluating this paper.

## References

- Allen, R. M., and H. Kanamori (2003), The potential for earthquake early warning in Southern California, *Science*, *300*, 786–789.
- Allen, R. M., and A. Ziv (2011), Application of real-time GPS to earthquake early warning, *Geophys. Res. Lett.*, *38*, L16310, doi:10.1029/2011GL047947.
- Böse, M., E. Hauksson, K. Solanki, H. Kanamori, and T. H. Heaton (2009), Real-time testing of the on-site warning algorithm in Southern California and its performance during the July 29, 2008 Mw 5.4 Chino Hills earthquake, *Geophys. Res. Lett.*, *36*, L00B03, doi:10.1029/2008GL036366.
- Böse, M., T. H. Heaton, and E. Hauksson (2012), Real-time Finite Fault Rupture Detector (FinDer) for large earthquakes, *Geophys. J. Int.*, *191*, 803–812, doi:10.1111/j.1365-246X.2012.05657.x.
- Böse, M., *et al.* (2013), CISM ShakeAlert: An Earthquake Early Warning Demonstration System for California, in *Early Warning for Geological Disasters—Scientific Methods and Current Practice*, edited by F. Wenzel and J. Zschau, pp. 49–69, Springer, Berlin Heidelberg New York, ISBN:978-3-642-12232-3.
- Brown, H. M., R. M. Allen, M. Hellweg, O. Khainovski, D. Neuhauser, and A. Souf (2011), Development of the ElarmS methodology for earthquake early warning: Realtime application in California and offline testing in Japan, *Soil Dyn. Earthquake Eng.*, *31*(2), 188–200, doi:10.1016/j.soildyn.2010.1003.1008.
- Colombelli, S., A. Zollo, G. Festa, and H. Kanamori (2012), Early magnitude and potential damage zone estimates for the great Mw 9 Tohoku-Oki earthquake, *Geophys. Res. Lett.*, *39* L22306, doi:10.1029/2012GL053923.
- Colombelli, S., R. M. Allen, and A. Zollo (2013), Application of real-time GPS to earthquake early warning in subduction and strike-slip environments, *J. Geophys. Res. Solid Earth*, *118*, 3448–3461, doi:10.1002/jgrb.50242.
- Cua, G., M. Fischer, T. Heaton, and S. Wiemer (2009), Real-time performance of the Virtual Seismologist earthquake early warning algorithm in Southern California, *Seismol. Res. Lett.*, *80*(5), 740–747.
- Kuyuk, H. S., and R. M. Allen (2013), Optimal seismic network density for earthquake early warning: A case study from California, *Seismol. Res. Lett.*, *84*(6), 946–954, doi:10.1785/0220130043.
- Kuyuk, H. S., R. M. Allen, H. Brown, M. Hellweg, I. Henson, and D. Neuhauser (2013), Designing a network-based earthquake early warning algorithm for California: ElarmS-2, *Bull. Seismol. Soc. Am.*, *104*(1), doi:10.1785/0120130146, in press.
- Lewis, M. A., and Y. Ben-Zion (2008), Examination of scaling between earthquake magnitude and proposed early signals in P waveforms from very near source stations in a South African gold mine, *J. Geophys. Res.*, *113*, B09305, doi:10.1029/2007JB005506.
- Olson, E., and R. M. Allen (2005), The deterministic nature of earthquake rupture, *Nature*, *438*, 212–215.
- Tsang, L., R. M. Allen, and G. Wurman (2007), Magnitude scaling relations from P-waves in Southern California, *Geophys. Res. Lett.* *34*, L19304, doi:10.1029/2007GL031077.
- Wurman, G., R. M. Allen, and P. Lombard (2007), Toward earthquake early warning in northern California, *J. Geophys. Res.*, *112*, B08311, doi:10.1029/2006JB004830.